International Journal of Engineering & Technology, 7 (4.26) (2018) 89-92

International Journal of Engineering & Technology

Website: www.sciencepubco.com/index.php/IJET

Research paper



Nanoscale Zinc Hydroxyapatite (ZnHA) Particles for Bone Tissue Engineering

Noorainol Faiz Noor Haris, Mardziah Che Murad* and Nik Rozlin Nik Masdek

Faculty of Mechanical Engineering, Universiti Teknologi MARA, 40450 Shah Alam, Selangor, Malaysia.
**Corresponding author E-mail: mardziah31@salam.uitm.edu.my*

Abstract

The aim of this paper is to discuss the differences in the structural properties of pure hydroxyapatite (HA) and zinc hydroxyapatite (ZnHA) nanoparticles. In this current research, nanosized HA and ZnHA were synthesised via chemical precipitation method with the use of ammonium dihydrogen phosphate, calcium oxide, zinc nitrate and distilled water. The temperature during synthesis process was maintained at 90 ^{0}C while the mixture stirred vigorously. The powders were then dried in the oven and calcined in a conventional high temperature furnace at 700 ^{0}C with varied soaking time of 2 and 3 hours for comparison purposes. The synthesised HA and ZnHA powders were subsequently characterised for thermal behaviour, phase composition and morphology examination using the Thermogravimetric Analyser (TGA), X-ray diffraction (XRD) and Field Emission Scanning Electron Microscopy (FESEM), respectively. From the XRD analysis, it was observed that the crystallinity of pure HA and ZnHA powders greatly increase after the calcination process. This can be indicated by the higher and rising intensities of the three main HA peaks in the XRD patterns. Even though the effect of soaking time during calcination did not seem very prominent from the diffraction spectra, its effect on the particle size can be seen clearly from the FESEM images. On the other hand, FESEM evaluation also shows that both HA and ZnHA nanoparticles are spherical in shape with the former powders having bigger size of particles.

Keywords: *Calcination; Chemical precipitation; Hydroxyapatite; Structural Properties; Zinc*

1. Introduction

Bone is a remarkable mineralized connective tissue. It has important roles in the body, such as for support and movement, protection of soft tissues and harboring of the bone marrow. Bone exhibits four types of cells that are: osteoblasts, osteocytes, osteoclasts and bone lining cells [1]. As we aged, bone will be more vulnerable to fractures because of damage or degenerative diseases. When this occurred, one of the treatments that can be done is through bone grafting. Bone grafting is a surgical operation which replaces missing bone with material either from the patient's own body, natural substitute, an artificial or can also be a synthetic. Bone grafting is practicable due to bone tissue ability to regenerate completely when they are provided with the space in which they have to grow [2]. As the natural bone grows, it will conventionally replace the graft material, developing into a fully integrated area of new bone.

Bone tissue engineering (BTE) aims is to induce a new functional bone tissue through the understanding of the bone itself [3]. Biomaterials is one of the components in BTE. Throughout the years, there have been continuous research on hydroxyapatite (HA) as a potential biomaterial in the medical industries [4]. Nanograin size HA is more desirable in clinical applications due to its improved properties over larger grain size HA. Nanocrystalline HA demonstrate better densification and sinterability, which also improves its fracture toughness and other mechanical properties [5].

HA is the main inorganic constituent of the bone and teeth [6-8]. Thus, it is known to be highly biocompatible and exhibit exceptional bioactive properties [5]. It can provide remarkable physicochemical bonds to the bone and later promote bone formation which are necessary for implant osseointegration. Osseointegration is needed as it can increase the implant efficiency and minimize the damages to surrounding tissues [9]. However, synthetic HA normally is low in strength which ultimately limits it use for load-bearing applications [5,10]. By substituting metal ion such as zinc into HA, the problem can be overcome or at least reduced as it is expected to improve the overall mechanical properties of HA.

Zinc (Zn) is considered as one of the essential ions in the human bone. It is an important mineral for the normal growth and the development of skeletal system [7]. Zn is also found to be present in the enamel of human teeth and bone [9]. Its deficiency is related with decrease in the bone density and therefore, in this present work, 10 mol% of Zn ion was substituted in the hydroxyapatite to observe its effects on the structural properties of HA.

2. Methods

In order to prepare pure HA and ZnHA, calcium oxide (CaO) and ammonium dihydrogen phosphate ($NH_4H_2PO_4$) was used as calcium and phosphate precursors, respectively while zinc nitrate hexahydrate ($Zn(NO_3)_2.6H_2O$) was used as a doping agent. All chemicals used were obtained from the research laboratory with no modifications made to them. The synthesis of pure HA and ZnHA powders were carried out using chemical precipitation method. In this technique, chemical precursors were added little by little into a beaker containing deionised water. The mixture was constantly stirred using magnetic stirrer for 3 hours at constant temperature of 90 °C on a hotplate. Crystallinity, morphology and

Copyright © 2018 Authors. This is an open access article distributed under the Creative Commons Attribution License, which permits unrestricted use, distribution, and reproduction in any medium, provided the original work is properly cited.

size distribution of the powders are believed to be strongly affected by the manipulation of the synthesis method parameters.



Fig 1: Crushing of the powders using pestle and mortar

For the zinc substitution, the chemicals were prepared with different $Zn(NO_3)_2.6H_2O$ solution which the number of reagents was calculated with assumption that Zn would substitute calcium and the (Zn+Ca)/P ratio was kept constant at 1.67. After 3 hours, the obtained precipitates were aged overnight allowing complete reaction to take place. It was then dried in hot air oven for 24 hours at temperature of 80 ^oC. Finally, it was ground into fine powders by using a pestle and mortar, crushing the initial aggregates formed which is shown in Fig. 1.

After crushing the solid aggregate into powder form, they were placed in a ceramic crucible and calcined at 700 ^oC with a heating rate of 5 °C/min in a high temperature furnace (THERMOLYNE 46100) as shown in Fig. 2. Soaking or holding time during the calcination were varied at 2 and 3 hours to observe any potential effect it has on the structural properties of the powders. The soaking stage in calcination process is normally done to 'mature' or to allow the heat-treated substances to become homogenous.



Fig 2: Calcination of as-synthesised powders

Thermal behaviour of the as-synthesised powders was studied using Thermogravimetric Analyser (TGA) (HITACHI, Japan). This analysis was conducted in a nitrogen atmosphere using alumina pan with a heating rate of 5 °C/min in the temperature ranging between 22 – 1192 °C. TG curves were plotted with the mass change in percentage (%) on the y-axis and temperature (T) on the x-axis.

Then, for the phase identification analysis, X-ray Diffraction (XRD, Rigaku, UltimaⅣ) method was used. XRD is primarily used to identify materials' phases and their different polymorphic forms, to distinguish between amorphous and crystalline material and also can be used to quantify the percentage of crystallinity of a sample. The diffraction spectra were recorded between 20^o and 50^o by using monochromatic CuKα (1.5406 Å) wavelength. The identification process was done by comparing the samples with the standard data of HA (ICDD File Card No. 01-074-9944) which can be obtained from the International Centre for Diffraction Data (ICDD) reference files.

For the morphological analysis, Field Emission Scanning Electron Microscopy (FESEM, Quanta Feg 450) was used. FESEM is an analytical technique that provides the elemental and topographical information at various magnifications with a virtually unlimited depth of field. To observe HA and ZnHA powders under the FESEM, they were first coated with platinum to ensure charging suppression. The average size of several particles was calculated by comparison to the scale bars of the figures using imageJ software.

3. Results and Discussion

3.1 Thermal Analysis of HA and ZnHA

The TGA curves for both as-synthesised HA and ZnHA powders are shown in Fig. 3. The total weight loss experienced by the powders are 19.45% and 17.5% for HA and ZnHA, respectively. The most pronounced mass loss can be seen occurred at around 22 – 250 °C (first stage), which is associated with the dehydration and evaporation of surface adsorbed water. The removal of interlayer adsorbed water along with condensation of phosphate group took place at around 250 – 600 °C. The mass loss at this stage is more gradual compared to the previous stage since it is more difficult to remove water from the lattice site.

At temperature between 600 – 800 °C, another mass loss occurred, which is most likely due to the phase decomposition of hydrogen phosphate. Around these temperatures, Zn ions are believed to have successfully replaced the Ca ions in the HA lattice site [11]. There is virtually no mass loss that took place from beyond 800 °C for both samples, implying that the powders have become fully crystallised and did not transform into another phase.

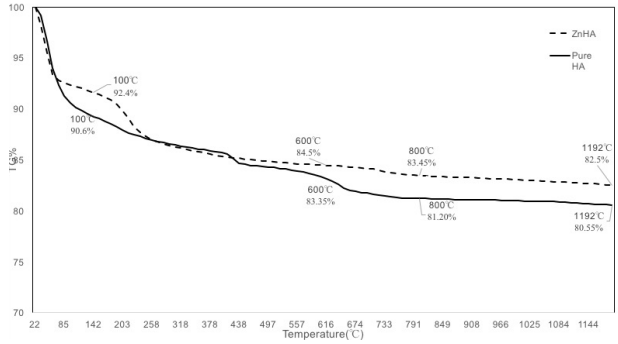


Fig. 3: TGA analysis of the 0 and 10 mol% ZnHA as-synthesised powders

3.2 Identification Analysis of HA and ZnHA

The comparative XRD diffractograms for pure HA and ZnHA are shown in Fig. 4 – Fig. 6. Fig. 4 displays the XRD patterns of the as-synthesised samples while Fig. 5 and Fig. 6 displays the diffractograms of the uncalcined and calcined powders with different soaking times (2 and 3 hours) at 700 °C.

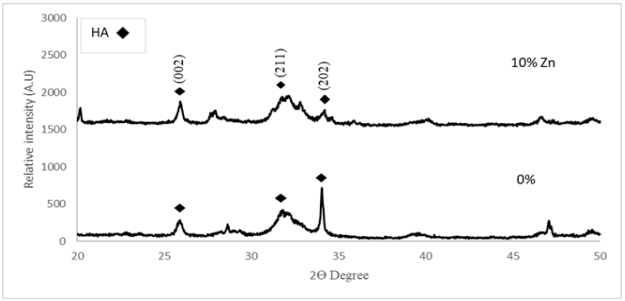


Fig. 4: XRD patterns of 0 and 10 mol% ZnHA samples before calcination process

From these figures, it can be deduced that all X-ray diffractograms of the samples closely matched with the reference HA (ICDD File Card No. 01-074-9944) even before the thermal process was carried out. The three main peaks of HA (211), (112) and (300) are clearly detected in the XRD patterns produced for HA and ZnHA. It is obvious that the intensity of diffraction peaks for both samples increases after the calcination process as indicated by the consistent sharper and narrower peaks, suggesting that it has better crystallinity. However, addition of Zn into HA is found to have affected the crystallinity level where the peaks are observed to become slightly less intense and broader. In other words, this decreasing crystallinity could reflect that the Ca ion has been replaced by the Zn ion in its lattice site. Based on the peak positions and intensities, it can be inferred that these materials do not contain any phase of impurities, confirming that addition of Zn did not alter the phase structure of HA.

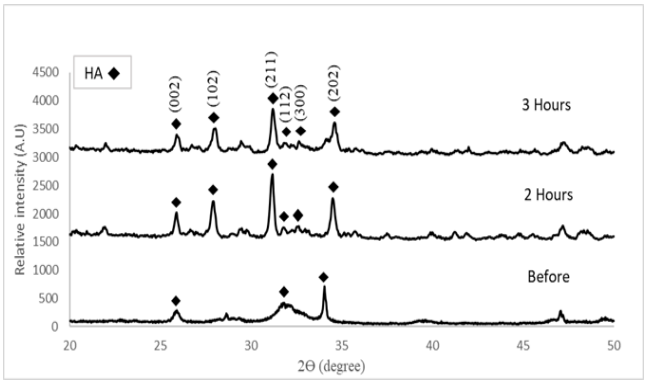


Fig. 5: XRD diffractograms of pure HA for three different conditions (before calcination, 2 hours and 3 hours soaking time).

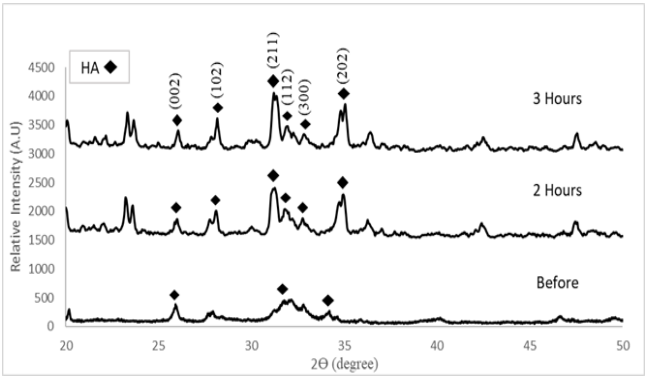


Fig 6: XRD diffractograms of ZnHA for three different conditions (before calcination, 2 hours and 3 hours soaking time).

XRD patterns of the materials developed in this research indicate that the soaking time during the calcination process, seems indiscernible in terms of its crystallinity, which agrees with the study made by Lima et al. [14]. Nonetheless, previous study has shown that the calcination temperature can also affect the level of crystallinity [12], but, it is not studied in this present work as the heat treatment was only conducted at a constant temperature of 700 °C.

From the XRD analysis, particle size of pure HA and ZnHA can be estimated by choosing the isolated HA peak (002) and then calculate them using the Scherrer equation [11]. The results are tabulated in Table 1.

$$D = \frac{K.\lambda}{\beta \cos\theta} \quad (1)$$

Where, λ is the Cu K_α radiation wavelength = 1.5406, β is the full width at half-maximum of the HA peak, θ is the diffraction angle, while K is a Scherrer constant (normally equated as 0.89 for spherical crystals).

Table 1: Particle size of pure HA

	Particle Size (nm)	
	Pure HA	ZnHA
Before calcination process	20.33	10.95
2 hours of soaking time	47.42	28.46
3 hours of soaking time	28.46	35.58

Table 1 also denotes interesting effects of the soaking time on both samples. For pure HA, longer soaking time causes the particle to become smaller but on the contrary for ZnHA, the effect is the opposite. This unique pattern is probably due to the presence of Zn ion which acts as a growth additive, hence promoting further particle coarsening during the soaking period. The evident difference in particle size of ZnHA can be seen from the FESEM images, in Fig. 7(d) and Fig. 9(e).

3.3 Morphological Analysis of HA and ZnHA

Fig. 7(a)-(e) exhibits the FESEM morphology of both powders, showing the particles have a distinct spherical shape. From these figures, it can also be concluded that thermal treatment or calcination of the HA powders could increase the size of the particles. This result coincides with the study that was carried out by Khoo et al. [12], where he claimed that the particle growth may be associated with the absorption of heat energy by the particles. The changing in particle size agrees with the calculated results from XRD data given in Table 1.

Using a scale bar from imageJ software, the particle size of HA and ZnHA were estimated. Since the particles are so small, they tend to agglomerate, hence it was unable to measure the dimension of an individual particle precisely. The size of the agglomerated particles, however, ranging from 50 – 200 nm. To improve contact reaction and stability at the artificial/natural bone interface, it is vital to ensure that the particle size of HA powders is in nanoscale. It is worth to note that the size of the apatite crystal in human bone is approximately 25 nm x 3 nm. Moreover, reduction in the particle size would significantly improve its mechanical stability, including hardness and material resistance properties [15].

It can also be seen from Fig. 7(b) that the pure HA nanoparticles are more tightly attached to each other compared to Fig. 7(c) due to shorter soaking time during calcination. This shows that by increasing the duration of soaking time, the particles formed will be less agglomerated and more dispersed. A study by Chandrasekar et al. [13] reported that the agglomeration of nanoparticles might be due to the Ostwald ripening, a phenomenon where smaller particles deposited on the larger ones to reach a more thermodynamically stable state.

4. Conclusions

HA and ZnHA nanopowders were successfully synthesised through chemical precipitation method which was confirmed after the characterisations through TGA, XRD and FESEM. XRD patterns show that HA is still the dominant phase in all samples even after Zn ion was substituted into it. Nonetheless, addition of Zn was discovered to have altered the crystallinity of HA. Broader peaks in the XRD patterns after the incorporation of Zn indicated the effect of the substitution. Calcination process, along with soaking time was found to have marginally affected the crystallinity and the particle growth of HA and ZnHA. Through FESEM examination, it can be observed that the particles of both powders were spherical in shape with dimension of the agglomerated particles ranging from 50 to 200 nm. As of now, resorbable bioceramics have been quite an interest in the biomedical industries. By conducting a more in-depth research in this area, the development process of the biomaterials could be more optimised and therefore, increasing its use and benefits for the industries in the future.

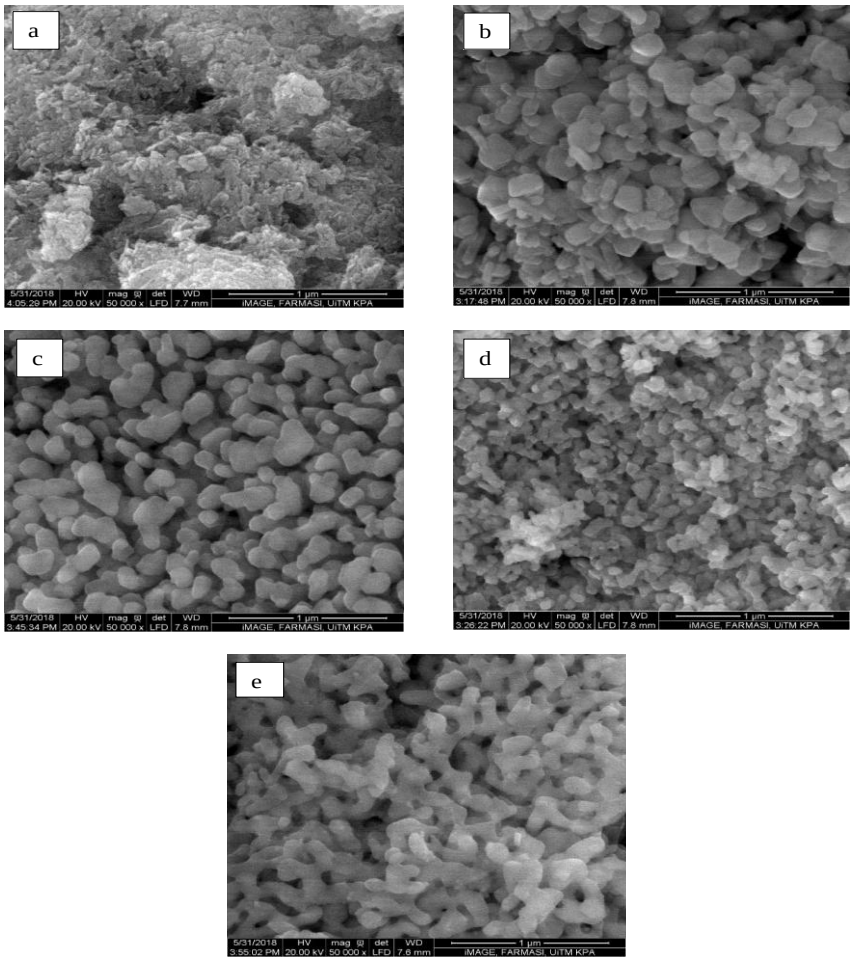


Fig. 7: FESEM micrograph of (a) pure HA before calcination process, (b) calcined pure HA with 2 hours soaking time, (c) calcined pure HA with 3 hours soaking time, (d) calcined ZnHA with 2 hours soaking time and (e) calcined ZnHA with 3 hours soaking time

Acknowledgement

The authors gratefully acknowledge Universiti Teknologi MARA (UiTM) and Institute of Research Management & Innovation (IRMI) for financial supports under Grant No. 600-IRMI/PERDANA 5/3 BESTARI (070/2018).

References

[1] R. Florencio-silva, G. Rodrigues, E. Sasso-cerri, M. J. Simões, P. S. Cerri, and B. Cells. Biology of bone tissue: Structure, function, and factors that influence bone cells. *Biomed Research International*, vol. 2015, 2015.

[2] M. Maas, U. Hess, and K. Rezwan. The contribution of rheology for designing hydroxyapatite biomaterials. *Curr. Opin. Colloid Interface Sci*., vol. 19, no. 6, pp. 585–593, 2014.

[3] A. R. Amini, C. T. Laurencin, and S. P. Nukavarapu. Bone tissue engineering: Recent advances and challenges. *Crit. Rev. Biomed. Eng*., vol. 40, no. 5, pp. 363–408, 2012.

[4] M. Prakasam, J. Locs, K. Salma-Ancane, D. Loca, A. Largeteau, and L. Berzina-Cimdina. Fabrication, properties and applications of dense hydroxyapatite: A review. *J. Funct. Biomater*., vol. 6, no. 4, pp. 1099–1140, 2015.

[5] Z. Evis and T. J. Webster. Nanosize hydroxyapatite: doping with various ions. *Adv. Appl. Ceram*., vol. 110, no. 5, pp. 311–321, 2011.

[6] P. Turon, L. del Valle, C. Alemán, and J. Puiggalí. Biodegradable and biocompatible systems based on hydroxyapatite nanoparticles. *Appl. Sci*., vol. 7, no. 1, p. 60, 2017.

[7] E. Boanini, M. Gazzano, and A. Bigi. Ionic substitutions in calcium phosphates synthesized at low temperature. *Acta Biomater*., vol. 6, no. 6, pp. 1882–1894, 2010.

[8] M. L. Popescu et al. Biocompatibility of hydroxyl-apatite thin films obtained by pulsed laser deposition. *Rev. Adv. Mater. Sci*., vol. 8, no. 2, pp. 164–169, 2004.

[9] D. Norhidayu, I. Sopyan, and S. Ramesh. Development of zinc doped hydroxyapatite for bone implant applications. *Int. Conf. Constr. Build. Technol*. 2008, no. 24, pp. 257–270, 2008.

[10] O. Victor, V. O. Ajibola, E. B. Agbaji, and A. A. Giwa. Synthesis of calcium hydroxyapatite nanocrystals using chemical precipitation technique: A Review. vol. 4, no. 1, pp. 39–54, 2015.

[11] C. M. Mardziah, N. R. N. Masdek, K. M. Hyie and I. Sopyan. Physicochemical Characteristics of MgHA derived via wet precipitation method. *Journal of Mechanical Engineering*, vol. 13 (2), pp. 10-20, 2016.

[12] W. Khoo, F. M. Nor, H. Ardhyananta, and D. Kurniawan. Preparation of natural hydroxyapatite from bovine femur bones using calcination at various temperatures. *Procedia Manuf*., vol. 2, no. February, pp. 196–201, 2015.

[13] A. Chandrasekar, S. Sagadevan, and A. Dakshnamoorthy. Synthesis and characterization of nano-hydroxyapatite (n-HAP) using the wet chemical technique. *Int. J. Phys. Sci*., vol. 8, no. 32, pp. 1639–1645, 2013.

[14] W. M. Lima et al. Effect of the calcination time of fish bones in the synthesis of hydroxyapatite. *Materials Science Forum*, vol. 498-499, pp. 600-605, 2005.

[15] S. M. Latifi, M. H. Fathi and M. A. Golozar. Preparation and characterization of hydroxyapatite-silica composite nanopowders. *International Journal of Modern Physics: Conference Series*, vol. 5, pp. 630-637, 2012.